Cationic lipid nanoparticle production by microfluidization for siRNA delivery

Xiaojing Liu, Badr Bahloul, René Lai Kuen, Karine Andrieux, Caroline Roques, Daniel Scherman

Cationic lipid nanoparticle production by microfluidization for siRNA delivery

Xiaojing Liu[a], Badr Bahloul[b], René Lai Kuen[c], Karine Andrieux[a], Caroline Roques[a], Daniel Scherman[a, d]

[a] Université de Paris, UTCBS, CNRS, INSERM, F-75006 Paris, France
[b] Laboratory of Pharmaceutical, Chemical and Pharmacological Drug Development LR12ES09, Faculty of Pharmacy, University of Monastir, Tunisia
[c] Université de Paris, CNRS, F-75006 Paris, France
[d] Corresponding author
Email address of corresponding author: daniel.scherman@u-paris.fr

Abstract

Microfluidization has been investigated as a new, scalable, and basic component saving method to produce cationic lipid nanoparticles, in particular for the delivery of short interfering RNAs (siRNAs). The design of experiment (DoE) allowed to reach optimized characteristics in terms of nanocarrier size reduction and low polydispersity. The structure of cationic liposomes and siRNA-lipoplexes was characterized. The optimized preparation parameters were identified as three microfluidization passages at a pressure of 10000 psi, with a thin film hydration volume of 4mL. Microfluidized liposomes mean size was 160nm, with a polydispersity index of 0.2 to 0.3 and a zeta potential of + 40mV to + 60mV. Positive versus negative charge ratio between the charges of the cationic lipid and the phosphate charges of the siRNAs is a key factor determining the structure and silencing efficacy of siRNA lipoplexes. At a (+/-) charge ratio of 8, a proportion of 88%

of the siRNA was associated to microfluidized lipoplexes, which remained stable for one month. These lipoplexes exhibited moderate cytotoxicity and gene silencing efficacy, which should be further optimized.

Keywords

Cationic liposome; lipoplex; siRNA; interfering RNA; gene silencing; microfluidization; thin film hydration; design of experiment.

Running Title: Microfluidized siRNA lipoplexes

1. Introduction

RNA interference (RNAi) is a promising strategy for the treatment of a large variety of disorders, including neurodegenerative diseases [1]. Short interfering RNAs (siRNAs) are 19-21 base pairs double-stranded RNAs that lead to the enzymatic degradation of a targeted mRNA through the RISC complex [2]. Cationic liposomes have been extensively used as siRNA delivery vectors, since they efficiently interact with negatively charged siRNAs and with the cell extracellular membrane, forming so-called lipoplexes [3]. Such lipoplexes are presently in clinical practice for the treatment of transthyretin amyloidosis (Patisiran) [4].

Microfluidization has been widely used to produce liposomal formulation [5], [6], that encapsulate nucleic acids [7], proteins [8] and drugs [9] exhibiting diverse physicochemical characteristics. The optimization of the manufacturing process of liposomal formulations can be obtained using a quality by design approach[10]. Microfluidization for the

preparation of cationic liposomes of appropriate size, distribution, and zeta potential might provide a scalable and economical platform for the delivery of siRNAs, which could meet the requirement for good manufacturing practice (GMP). The high pressure and shear force of the microfluidization process effectively decrease the size and polydispersity index (PDI) of nanoparticles. Besides, the limited number of parameters involved in microfluidization optimization, i.e. pressure and number of passages, saves development costs [11], as compared to other techniques such as sonication (which depends on time, amplitude, pulse-on/pulse-off time, ice replenish frequency), and high-pressure homogenization (which depends on pressure, number of cycles, and flow) [12], [13].

At optimized size and zeta potential, cationic liposomes have been shown to efficiently encapsulate siRNA and functionally in a large number of cells in vitro, and also in vivo in liver by intravenous administration [14], [15]. In the present study, we have used the thin film hydration method to form cationic lipids multilamellar vesicles, which were subsequently microfluidized in order to obtain reduced small unilamellar vesicles. We used a three lipid composition containing the cationic lipid 2-{3-[Bis-(3-amino-propyl)-amino]-propylamino}-N-ditetradecyl carbamoyl methyl-acetamide (DMAPAP), a neutral colipid, and a PEG-lipid. The DMAPAP lipid contains three positive amine charges in its head group and has proved its efficiency for lipoplexes formulation and efficient siRNA delivery in a series of precedent studies [16], [17]. The most important physicochemical lipoplexes characteristics (mean size, polydispersity and zeta potential value) were optimized by varying experimental conditions and using a design of experiment (DoE)

approach. The siRNA-lipoplexes encapsulation efficiency was evaluated, and the cytotoxicity and silencing efficacy were tested in vitro.

2. Materials and Methods

2.1 siRNA.

Luciferase siRNA (CUUACGCUGAGUACUUCGA sense) and scramble siRNA (UUCUCCGAACGUGUCACGU sense) were purchased from Eurogentec.

2.2 Liposomes preparation by thin film hydration method.

The cationic lipid 2-{3-[Bis-(3-amino-propyl)-amino]-propylamino}-N-ditetradecyl carbamoyl methyl-acetamide or DMAPAP (Figure 1) was synthesized as previously described [16,17]. The helper lipid DOPE (1,2-dioleoyl-sn-glycero-3-phosphoethanolamine) and the DSPE-PEG 2000 lipid (1,2-diacyl-sn-glycero-3-phosphoethanolamine-N-[methoxy (polyethylene glycol)-2000] were purchased from Avanti Polar Lipids (Figure 1). The DMAPAP, DOPE and DSPE-PEG 2000 lipids were dissolved in chloroform at molar ratio 50/45/5 by reference to previous works [18-20], evaporated under vacuum at 40°C for 1 hour to form a thin film, and left to dry for 2 hours. The film was then hydrated with different volumes of Milli-Q water overnight at room temperature.

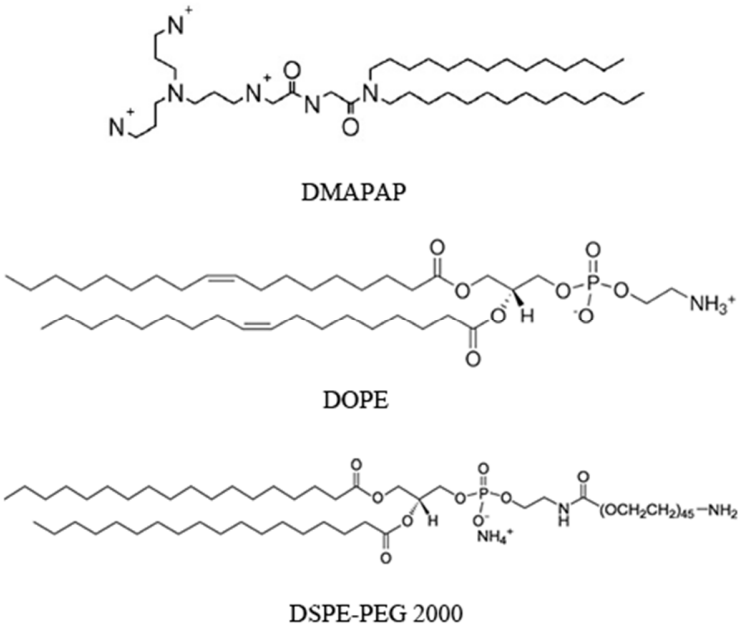

Figure 1. Molecular structures of DMAPAP, DOPE, DSPE-PEG2000 lipids [20] , [28], [36].

2.3 Liposomes' size reduction

2.3.1 Extrusion method

The hydrated liposomal suspension (hydration volume 4mL) was passed through polycarbonate filters of 0.4 μm pore size for 10 passages, and of 0.2 μm for 10 additional passages in a Mini-Extruder (Avanti Polar Lipids) at room temperature.

2.3.2 Microfluidization method

After hydration, the liposomal suspension was injected into a microfluidizer (LV1, Microfluidic Corp., Newton, MA, USA) by 5ml/10ml syringe in a Y-type chamber [21] and processed with various microfluidization pump pressure, and number of passages conditions. Cooling coil temperature was maintained at 0°C in ice during the process.

2.4 Selection of factors and responses in the experimental design. X1 pressure (ranging from 5000 psi to 20000 psi) and X2 number of passages (ranging from 1 to 5)

were selected according to the microfluidizer operation guide [21]. The factors ranges were set up based on preliminary results, on the targeted value of response, and on reference to the literature [22]. The thin film hydration volume was included as variable X3 (ranging from 4ml to 16ml), since it was observed in preliminary results to be a key factor determining liposomes size and PDI, in agreement with the literature [23,24]. Other factors for thin film hydration such as lipid composition and concentration, vacuum pressure, evaporation time, heating bath temperature, hydration time, and rotation speed were fixed at a constant value, based on our previous results [18-20]. Three responses: Y1 (size in the present text), Y2 (polydispersity index PDI) and Y3 (zeta potential), were selected to define the liposomes and lipoplexes characteristics. Target values of responses were optimized for effective delivery and stability of nanocarrier [25-27] (Table 1).

Table 1. Factors and responses used in the design of experiment.

	Level (coded)	
	Low (-1)	High (+1)
Factors		
X1: Pressure (psi)	5000	20000
X2: Number of passages	1	5
X3: Hydration volume (mL)	4	16
Responses	**Target value**	
Y1: Size (nm)	150	
Y2 PDI	0.2-0.3	
Y3: Zeta potential (mV)	+40-+60	

2.5 Modelization.

Customized design of experiment with the three factors X1 (pressure), X2 (number of passages), and X3 (hydration volume) was performed. The analysis and optimization

118 procedure were conducted using the statistical software STATGARPHICS Centurion
119 (Version 15.1.02, USA). The polynomial equation used was: Y = b0 + b1X1 + b2X2 +
120 b3X3 + b4X1X2 + b5X2X3 + b6X1X3 + b7X12 + b8X22 + b9X32, linking the
121 dependent variables, Y1 and Y2, to the independent variables, X1, X2 and X3, and
122 wherein b0 was the intercept and b1 to b9, were the regression coefficients. We used a 2-
123 levels, 3-factors design as a model to improve the quality of predicted results using the
124 preliminary preformulation data. Our approach involved the use of prior results to build a
125 common design customized for the optimization procedure (Table 2). The optimization
126 procedure was performed using a desirability function with the aim to obtain an optimum
127 liposome formulation characterized by a 150 nm target size and a + 60 mV zeta potential.
128 Validation tests were carried out by triplicates of each experiment conditions of
129 optimized batch and optimum value obtained by math model.

130 **Table 2.** Experimental matrix of customized design of experiment.

Run	X1	X2	X3
1	20000	1	16
2	20000	3	16
3	20000	5	16
4	15000	1	16
5	15000	3	16
6	15000	5	16
7	5000	1	16
8	5000	3	16
9	5000	5	16
10	20000	1	4
11	20000	3	4
12	20000	5	4
13	15000	1	4
14	15000	3	4
15	15000	5	4
16	10000	1	4
17	10000	3	4
18	10000	5	4
19	20000	1	8
20	20000	3	8
21	20000	5	8

22	15000	1	8
23	15000	3	8
24	15000	5	8
25	5000	1	8
26	5000	3	8
27	5000	5	8

2.6 Lipoplexes preparation and characterization. Lipoplexes were formulated by mixing in 150 mM NaCl an equal volume of cationic liposomes and of siRNA solution (anti-luciferase or scramble siRNA as a negative control), vortexing for 1 minute and allowing to form lipoplexes for at least 30 min at room temperature. Different charge ratios were studied and calculated using the molar ratio of positive charges (3 positive charges per molecule of DMAPAP) to negative charges of siRNA (3.03 nmole of negative phosphate charges/µg of siRNA) [16, 18, 28].

Size and zeta potential were determined by dynamic light scattering (DLS) using a Zetasizer Nano ZS (Malvern Instruments). Blank liposomes (final lipid concentration 0.1 mM) and lipoplexes (final siRNA concentration 37.5nM) were suspended in Milli-Q water for short term storage. The DLS condition was set up as: water dispersant (viscosity, refractive index), detector position 173°, at temperature 25°C.

For transmission electron microscopy (TEM), a drop (20 µl) of liposomes or lipoplexes dispersion (siRNA concentration 375.9 nM) was first applied onto a Formvar/carbon 200 mesh copper grid for 2 min, blotted with filter paper. Then a drop (20 µl) of 1% uranyl acetate (UAC) was applied on the copper grid for 2 min, blotted with filter paper and dried for 10 min. Analyses were performed on a microscope JEOL, JEM 100S as described [18],[19].

2.7 Liposomes/lipoplexes storage and stability. Cationic liposomes and lipoplexes suspensions were stored at 4 °C in 1.5 mL Eppendorf tubes. The size, PDI and zeta

potential were measured by DLS within 3 days and weekly within one month after formulation.

2.8 Gel retardation assay. Lipoplexes were prepared as described above (0.3 µg siRNA/sample/10 µl) at different charge ratio. Samples were mixed with 2 µl dye (6X) and electrophoresed on 1.5% agarose gel in Tris-Acetate-EDTA (TAE 1X) buffer at 80 V for 30 min [18]. Then, the gels were placed into ethidium bromide (BET) bath for 15 minutes and free siRNA band was visualized on UV transilluminator. The digital images were acquired using Bio-Capt Version 12.6 for Windows and were analyzed by image J software.

2.9 Cell culture. Mouse melanoma cells (B16-F10, ATCC CRL6475) were grown on DMEM with glutamax (Gibco), 10% fetal calf serum (Sigma-Aldrich), streptomycin (100 µg/ml from ThermoFisher scientific), and selection antibiotic geneticin (2 mg/ml, Gibco). Cells were trypsinized and passaged twice weekly for transfection.

2.10 Cytotoxicity determination. B16-luc cells were plated on 96-well plates at a density of 4,000 cells per well in 100 µl of culture medium. After 24 hours plating, 100 µl of lipoplexes were prepared as described above, mixed with culture medium, and added to the cells in triplicate experiments. After a 48h exposure period, cell viability was assayed using the MTT test as previously described [19]. Control wells with DMEM and 150 mM NaCl with MTT were run to subtract background absorbance. Results were expressed relative to non-transfected cells.

2.11 Gene silencing efficiency. Cell transfection was performed as above. Transfection medium was replaced by fresh medium at 24 hours after transfection and incubated for an additional 24 hours. The transfected cells were washed twice with PBS and lysed with

200 µl cell culture lysis reagent (Promega). The luciferase assay was carried out according to the manufacturer's protocol. Light emission from luciferase activity was measured in white 96-microwell plates using a Wallac Victor2 microplate reader equipped for luminescence. Total protein concentration was determined using the Pierce BCA assay (Thermo Scientific). The results were calculated in cps (count per second), normalized to the total protein concentration of each sample, and expressed relatively to non-transfected control cells [19].

3. Statistical analysis and computation. All results were expressed by mean value ± standard deviation (SD). The adequacy of the polynomial model for the responses was verified by ANOVA, multiple correlation (R^2) and Durbin-Watson (DW) statistical tests. The desirability function D was calculated by the STATGARPHICS CENTURION (Version 15.1.02, USA) software. Two-ways ANOVA multiple comparisons and Bonferroni test were used to test the significance between groups by Prism 9 (version 9.0.0, GraphPad).

4. Results and discussions

4.1 Customized design of experiments (DoE)

Twenty-seven runs were performed for design of experiment analysis. The observed results are shown in Table 3. Liposome's size varied from 96.75 nm to 310.5 nm, PDI from 0.17 to 0.45, and zeta potential from 54.2mV to 86.4 mV. The polynomial equations relating the responses Y1, Y2, Y3 and independent variables are listed in Table 4. The adequacy of this model was verified by ANOVA, multiple correlation (R^2) and Durbin-Watson (DW) statistical tests. The P values of separated effects for responses Y1, Y2 and Y3 were found to be less than 0.05. The Durbin-Watson (DW) statistical tests for size and

198 PDI were used in order to determine significant correlations between the Table 3 data.
199 When P values were less than 0.05, there was an indication of serial correlation at the
200 0.05 significance level. R^2 values for responses were > 80%. Thus, it can be concluded
201 that the responses fitted well the quadratic model.

202 **Table 3**. Experimental domain and observed values of the customized DoE analysis.

Run	X1 Pressure (psi)	X2 Passages	X3 Hydration volume (mL)	Y1 Size (nm)	Y2 PDI	Y3 Zeta potential (mV)
1	20000	1	16	297.5	0.42	80.7
2	20000	3	16	214.4	0.23	83
3	20000	5	16	191.6	0.25	76.1
4	15000	1	16	271.2	0.35	70.5
5	15000	3	16	310.5	0.34	73
6	15000	5	16	283.8	0.31	72
7	5000	1	16	307	0.31	69.8
8	5000	3	16	298.8	0.31	73
9	5000	5	16	286.23	0.35	80.4
10	20000	1	4	134	0.37	62.7
11	20000	3	4	176.4	0.3	68
12	20000	5	4	168.1	0.45	63.1
13	15000	1	4	96.75	0.39	54.2
14	15000	3	4	147	0.36	63.3
15	15000	5	4	242.9	0.32	63.7
16	10000	1	4	167.7	0.2	61.9
17	10000	3	4	164.2	0.2	59.6
18	10000	5	4	162.5	0.23	58.6
19	20000	1	8	175.5	0.22	69.7
20	20000	3	8	175.9	0.21	86.4
21	20000	5	8	159.8	0.19	82.6
22	15000	1	8	178.4	0.21	65.8
23	15000	3	8	169.1	0.17	75.1
24	15000	5	8	167.9	0.18	78.8
25	5000	1	8	178.2	0.23	67.7
26	5000	3	8	194.5	0.25	70.9
27	5000	5	8	197.8	0.24	77.3

203

Table 4. Polynomial equations for the responses.

Y1	$Y1 = 11.8986 + 0.0109046X1 + 28.383X2 + 9.19764X3 - 3.05845E\text{-}7X1^2 - 0.000538838X1X2 - 0.000346733X1X3 + 0.0705556X2^2 - 2.24116X2\ X3 + 0.612531X3^2$
Y2	$Y2 = 0.386851 + 0.00000307474X1 - 0.00512917X2 - 0.0487927X3 + 3.9516E\text{-}10X1^2 - 0.00000146083X1X2 - 6.93261E\text{-}7X1X3 + 0.006X2^2 - 0.00166944X2X3 + 0.00319514X3^2$
Y3	$Y3 = 34.0186 - 0.00127128X1 + 6.57042X2 + 6.10165X3 + 7.8605E\text{-}8X1^2 - 0.00010275X1X2 + 1.58306E\text{-}7X1X3 - 0.590278X2^2 - 0.0433333\ X2X3 - 0.245029X3^2$

4.2 Coefficient estimates and standardized main effects

Using our preliminary results, the coefficient estimates with their corresponding p values in the form of polynomial equations were deduced in Table 5. The respective weight of factors (X1, X2, X3) and their interactions on the responses (Y1, Y2, Y3) were calculated by the polynomial equations of Table 4 and were shown in a Pareto chart (Figure 2). It can be deduced from the Pareto chart that the main and quadratic effects of hydration volume, the main effect of the number of passages, and the interaction between these two factors (X2, X3, X2X3, $X3^2$) had the most important weight of all factors on Y1, Y2 and Y3. In Table 5, Y1 (size) was significantly affected by the synergistic effect of X2 (number of passages) and the interaction X3X2 (number of passages and hydration volume) with p values of 0.0499 and 0.0035, respectively.

224 **Table 5.** Standardized main effects of the factors and their corresponding p values on the Y1, Y2
225 and Y3 responses.
226

Source	Factors	Size Y1		PDI Y2		Zeta Y3	
		Estimate	P-Value	Estimate	P-Value	Estimate	P-Value
A: Pressure	X1	0.0109046	0.7561	0.0307	0.1762	-0.00127128	0.0848
B: Passages	X2	28383	0.0499*	-0.00512917	0.7813	657042	0.0287*
C: Hydration volume	X3	919764	0.1483	-0.0487927	0.0088*	610165	0 .000*
AA	$X1^2$	-3.06E-07	0.2235	3.95E-10	0.4781	7.86E-08	0.0475*
AB	X1X2	-0.00053884	0.3683	-0.0146	0.281	-0.00010275	0.2624
AC	X1X3	-0.00034673	0.1235	-6.93E-07	0.1681	1.58E-07	0.9962
BB	$X2^2$	0.0705556	0.9805	0.006	0.3618	-0.590278	0.1901
BC	X2X3	-224116	0.0035*	-0.00166944	0.2781	-0.0433333	0.6723
CC	$X3^2$	0.612531	0.126	0.00319514	0.0017*	-0.245029	0.0006*

227
228
229

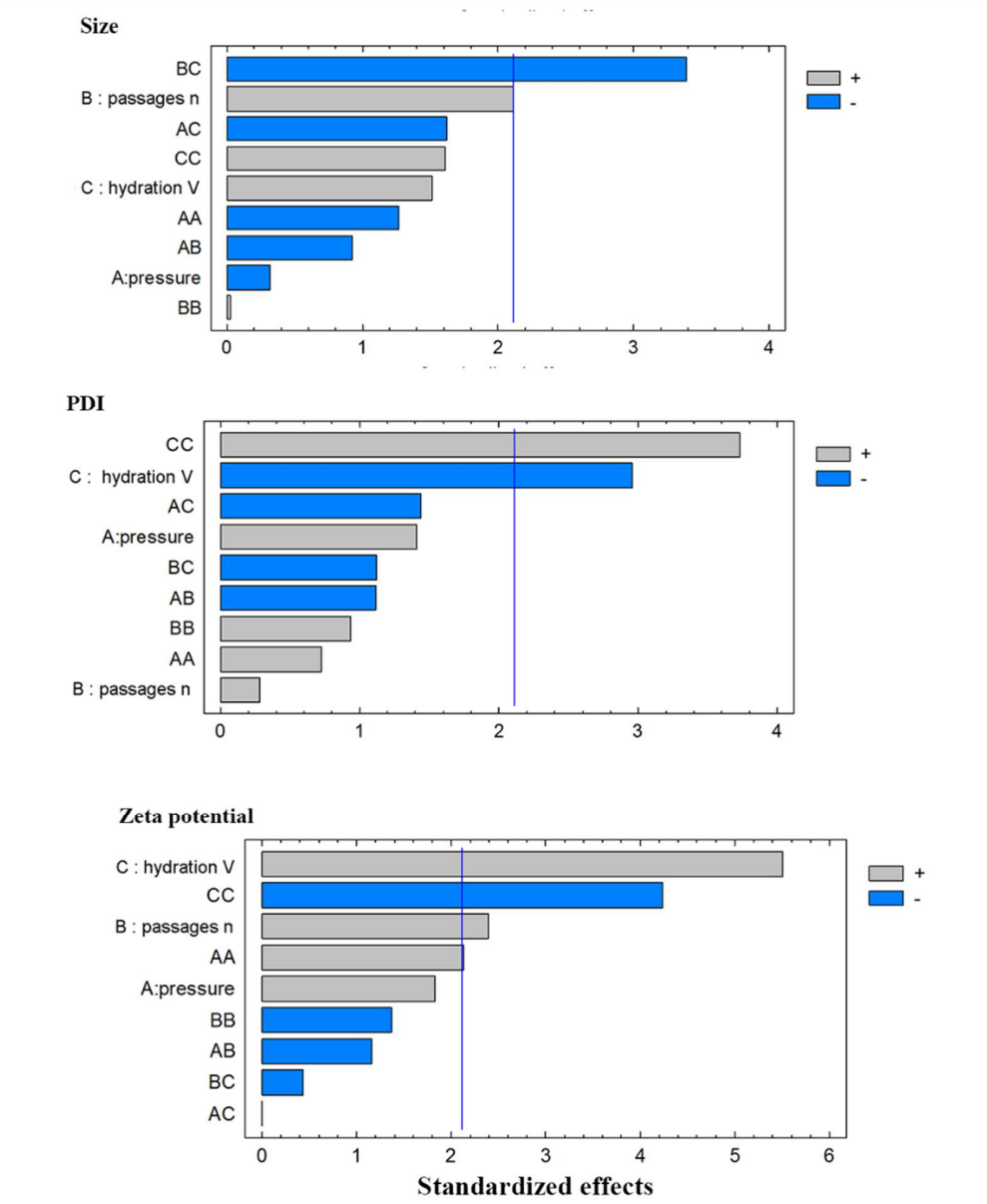

Figure 2. Standard Pareto chart showing the effect of the independent variables X1, X2 and X3 and their combined effects on Y1 (size); Y2 (PDI); and Y3 (zeta potential). (Colored)

4.3 Influence of pressure and number of passages on liposomes size

The effect of X1 (pressure), X2 (number of passages) and their interaction on Y1 (size) at a fixed level of X3 (hydration volume) is given in Figure 3. At low number of passages, Y1 increased from 138 nm to 186 nm when the X3 increased from 2ml to 8 ml. However, at high number of passages, Y1 did not increase significatively, showing that the effect of

the hydration volume is only detectable for a low number of passages, and suggesting that hydration volume is the key factor influencing liposome size. The reason could be that the number of bilayers of the multilamellar vesicles (MLVs) formed during the film hydration spontaneous process can be tuned by varying the initial properties of the lipid droplet [29], such as evaporation/hydration volume, flask size, lipid composition and concentration [30,31]. These factors also determine the final size of liposomes during the subsequent microfluidization.

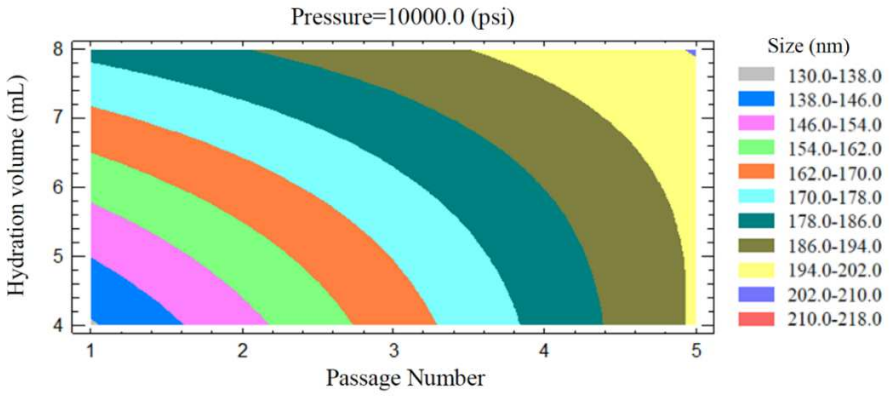

Figure 3. Response surface plots showing the effect of X2 (passage number) and X3 (hydration volume) on response Y1 (size). (Colored)

4.4 Influence of number of passages and hydration volume on zeta potential

The effect of X2 (number of passages) and X3 (hydration volume) and their interaction on Y3 (zeta potential) at a fixed X1 pressure (10000 psi) was shown in Figure 4. At low X2 value, Y3 increased from 54mV to 68 mV when X3 increased from 4 ml to 8 ml. Similarly, at high value of X2, Y3 increased from 60mV to 72 mV when X3 increased from 4ml to 8 ml.

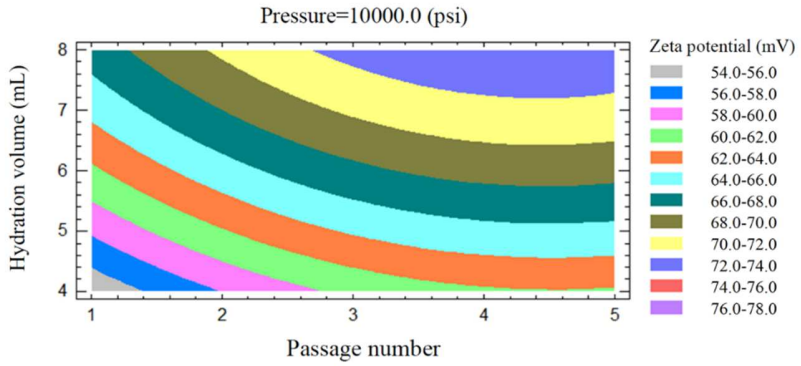

Figure 4. Response surface plots showing the effect of X2 (number of passages) and X3 (hydration volume) on response Y3 (zeta potential). (Colored)

4.5 Optimization using a desirability function and validation

This procedure helped to determine the combination of experimental factors which simultaneously optimized several responses by maximizing a desirability function. The target value for size was 150 nm and for zeta potential was 60 mV. The scale of the desirability function ranged from D = 0 for a completely undesirable response to D = 1 if the response corresponds to the most desirable value. The desirability function calculated at each point in the design is summarized in Table 6. Maximum desirability was achieved at run 17 with a satisfaction rate of 92.14%. The predicted factor combinations to achieve optimum value are shown in Table 7.

Triplicate validation tests showed that the experimental condition predicted by the mathematical model did not reach the size value and narrow distribution required for the cationic lipid nanoparticle (data not shown). The run 17 experiment was observed to be closer to target size and chosen for in vitro silencing efficacy assay.

In the present work, the size of microfluidized-cationic liposomes was larger than that observed with other types of cationic liposomes prepared under similar conditions (pressure and number of passages) [22,32]. This discrepancy could be explained by the fact

that the DMAPAP molecule has three positive charges and thus possesses a larger headgroup volume and identical lipidic moiety volume, as compared to DOTAP or DC-Chol, which carry only one positive charge in their headgroup.

Table 6. Predicted and observed desirability at each point of the design.

			Predicted	*Observed*
Row	*size*	*zeta*	*Desirability*	*Desirability*
1	297.5	80.7	0.2058	0.1081
2	214.4	83.0	0.3221	0.3746
3	191.6	76.1	0.4817	0.6130
4	311.0	73.0	0.0000	0.0000
5	310.5	73.0	0.2318	0.0133
6	283.8	72.0	0.3896	0.2353
7	307.0	69.8	0.0000	0.0624
8	298.8	73.0	0.0728	0.1299
9	286.23	80.4	0.1981	0.1694
10	134.0	66.7	0.7558	0.7145
11	176.4	68.0	0.8845	0.7922
12	168.1	63.1	0.8193	0.8856
13	96.75	54.2	0.7796	0.0178
14	147.0	63.3	0.8980	0.9235
15	242.9	63.7	0.7866	0.5177
16	167.7	61.9	0.3901	0.9004
17	164.2	59.6	0.9242	0.9179
18	162.5	58.6	0.7757	0.8749
19	175.5	69.7	0.6947	0.7737
20	175.9	86.4	0.6029	0.0000
21	159.8	82.6	0.6333	0.5347
22	178.4	65.8	0.7518	0.8100
23	169.1	75.1	0.6624	0.7128
24	167.9	78.8	0.6413	0.6370
25	178.2	67.7	0.8389	0.7883
26	194.5	70.9	0.6762	0.6795
27	197.8	77.3	0.5805	0.5687

Table 7. Experiment conditions and validation of run 17 and optimum value (triplicates).

	Pressure (psi)	Passage number	Hydration volume (mL)	Size (nm)	PDI	Zeta potential (mV)
Run 17	10000	3	4	160±9	0.2±0.0	52±9
Optimum	9543	1	5.3	213±53	0.3±0.1	48±10

4.6 Physicochemical characteristics of liposomes and lipoplexes

The size and PDI of blank liposomes and lipoplexes were similar, and the lipoplexes zeta potential was lower than that of blank liposomes, likely because of the blank cationic liposome complexation with the negatively charged siRNA (Figure 5 and Table 8). The morphology of blank liposomes and lipoplexes was studied by TEM. Blank liposomes were spherical with a blank core. Lipoplexes at charge ratio 8 exhibited unsmooth surface and dense core, indicating that the siRNA molecules have been complexed with liposomes and formed a structure neither lamellar nor hexagonal, thus different from our previous formulations and from the literature [18-20, 33, 34] (Figure 6).

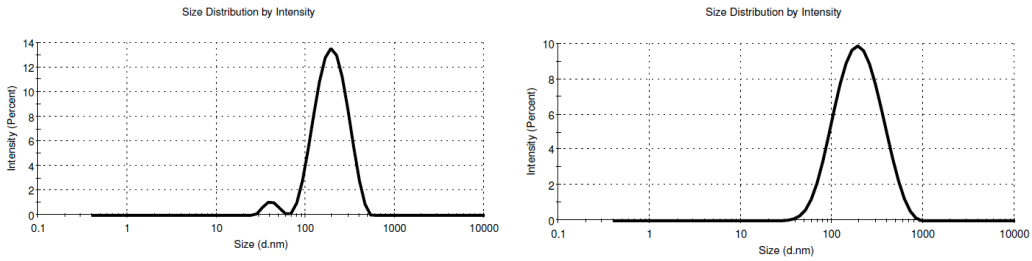

Figure 5. Size and PDI of blank liposomes (left panel) and lipoplexes (right panel) of charge ratio 8 as assessed by dynamic light scattering (DLS).

Table 8. Average value of size, PDI and zeta potential of blank liposomes and lipoplexes. (Mean ± SD of three separate experiments)

Formulations	Size (nm)	PDI	Zeta potential (mV)
Blank liposome	160±9	0.28±0.0	52±9.8
Lipoplexe charge ratio 8	165±1	0.21±0	36±3.3

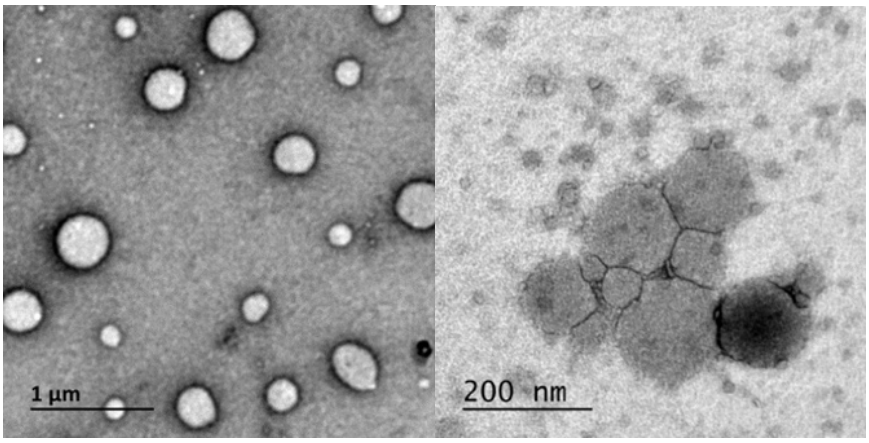

Figure 6. TEM micrographs of blank liposomes and siRNA-lipoplexes. TEM micrographs of blank liposomes (left, spherical shape) and siRNA-lipoplexes at (+/-) charge ratio of 8 (right, unsmooth surface and dense core) were performed using negative staining.

4.7 Gel retardation assay

Nine samples were prepared and electrophoresed on agarose gel: free siRNA, blank liposomes, and lipoplexes with a charge ratio ranging from 0.5 to 10. The charge ratio between cationic lipid positive amines and siRNA negative phosphate was calculated as described in the Methods section. The result illustrated the efficient siRNA encapsulation at a charge ratio of 8, with encapsulation yield of 88%, and at charge ratio of 10, with complete encapsulation (Figure 7).

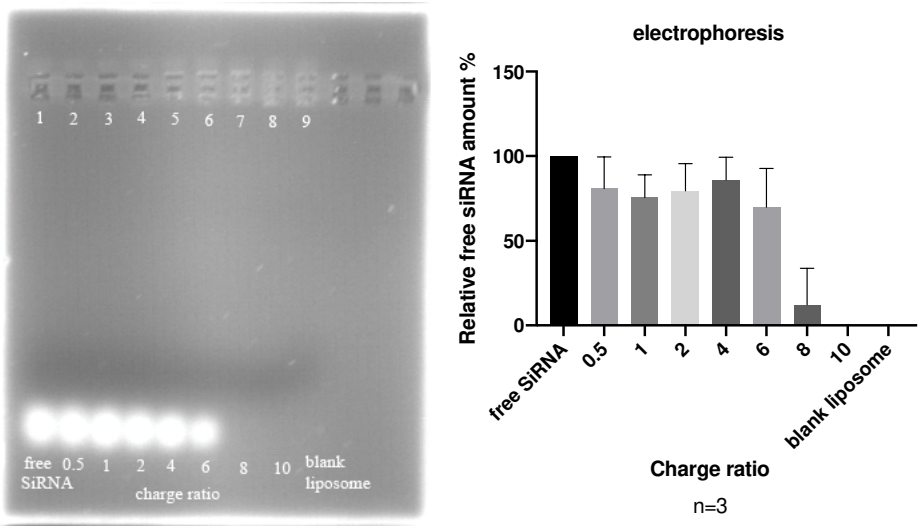

Figure 7. Gel retardation assay of lipoplexes. Lipoplexes with different charge ratio from 0.5 to 10 (0.3 µg siRNA/lane), free siRNA and blank liposomes were tested. Samples were deposited onto 1.5% agarose gel and the electrophoresis was run at 80 V for 30 mins. Free siRNAs were visualized following incubation with BET through fluorescence under UV light. (Charge ratio = nmol of cationic lipid (DMAPAP) /ug of siRNA).

4.8 Stability

The stability of lipoplexes prepared either by microfluidization (at different charge ratios from 0.5 to 8) or by extrusion (charge ratio of 4 as in previous work from our team) was assessed over one month. The extruded lipoplexe preparation was stable in terms of size, PDI, and zeta potential. The microfluidized lipoplexes were stable only at the higher charge ratio of 8. Size, PDI of these two formulations were similar, zeta potential of microfluidized lipoplexes at charge ratio 8 was higher at 37.0mV compared to extruded lipoplexes, finally decreased to 12.2mV over one month (Figure 8). At charge ratio 10, zeta potential revealed unacceptable variability, particle sediment and aggregation (data not shown), indicating that the high charge ratio 10 resulted in instability.

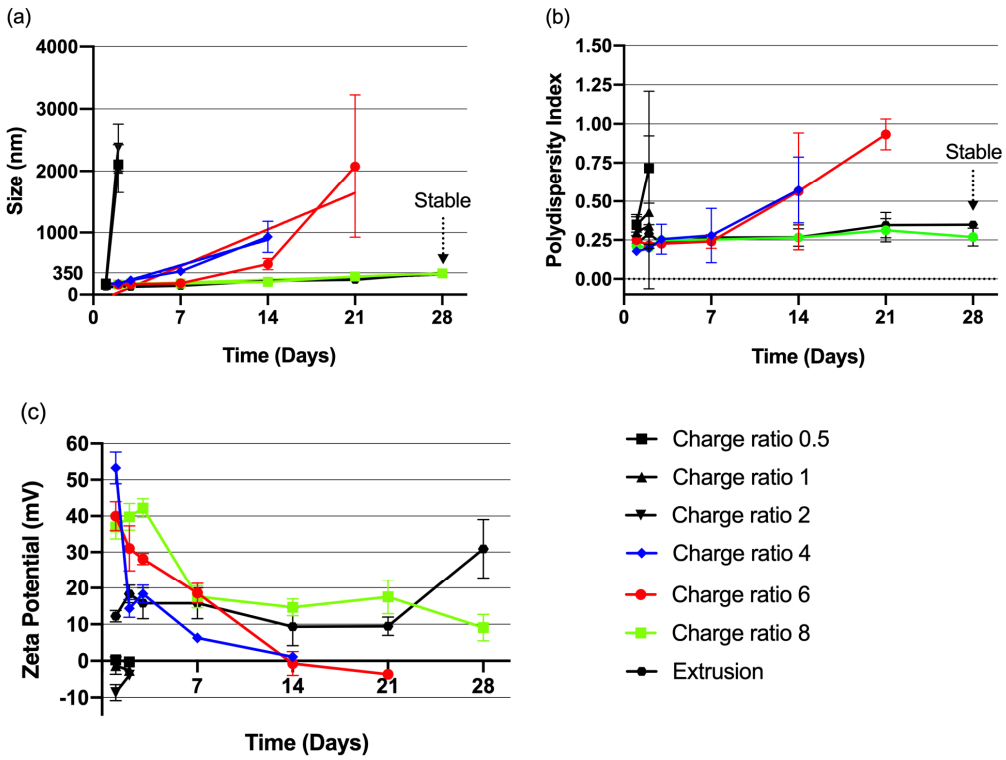

Figure 8. Lipoplexes stability assessment. Stability of microfluidized lipoplexes with charge ratio range 0.5 to 8 in terms of size (a), PDI (b) and zeta potential (c) over one month. Extrusion lipoplexes had a charge ratio of 4. (Colored)

4.9 Cytotoxicity and silencing efficiency

Cytotoxicity was evaluated by MTT test at anti-luciferase siRNA concentration ranging from 10 nM to 150 nM. For siRNA concentrations of 10 nM to 20 nM, cell viability attained 98%-100%. However, when the siRNA concentration increased up to 150 nM, cell viability decreased down to 50%. Microfluidized lipoplexes with a charge ratio of 4 to 8 and extrusion reference lipoplexes (charge ratio 4) presented approximately the same level of cytotoxicity (Figure 9a).

For silencing activity assessment, a luciferase assay was performed on a reporter cell line [18], [38]. With microfluidized lipoplexes at a siRNA concentration of 44 nM at a charge ratio of 8, we observed a 51% of inhibition of luciferase (LUC) gene expression, with

353 30% cytotoxicity, against only 25% of Luc gene expression observed when using the
354 scrambled unmatched siRNA (Figure 9b). This difference was statistically significant.
355 At a siRNA concentration of 66 nM, the silencing of Luc expression reached 66%, with
356 30% cytotoxicity. However, since 52% Luc expression was observed when using the
357 scramble siRNA, it can be deduced that, at this high siRNA concentration, the non-
358 specific effect of siRNA lipoplexes became predominant. The LUC expression silencing
359 observed with microfluidized lipoplexes at charge ratios 4 and 6 was not significant (data
360 not shown). A higher silencing efficacy has been described in previous studies and from
361 the literature. It can be suggested that the present formulation could be improved by
362 reducing the PEG lipid content to less than 5% [18],[19],[22],[28].
363

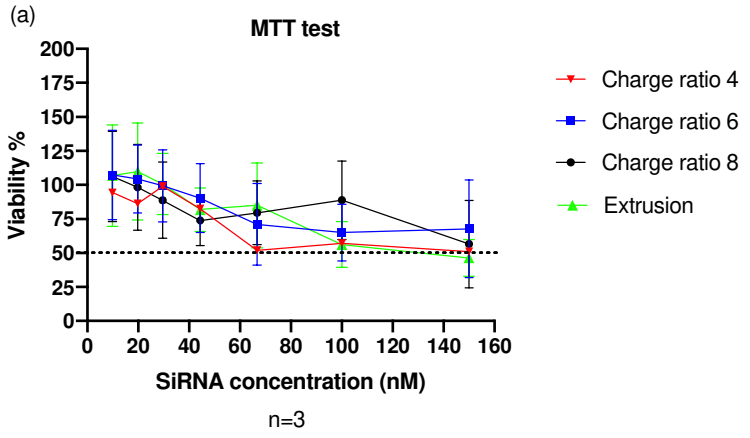

364

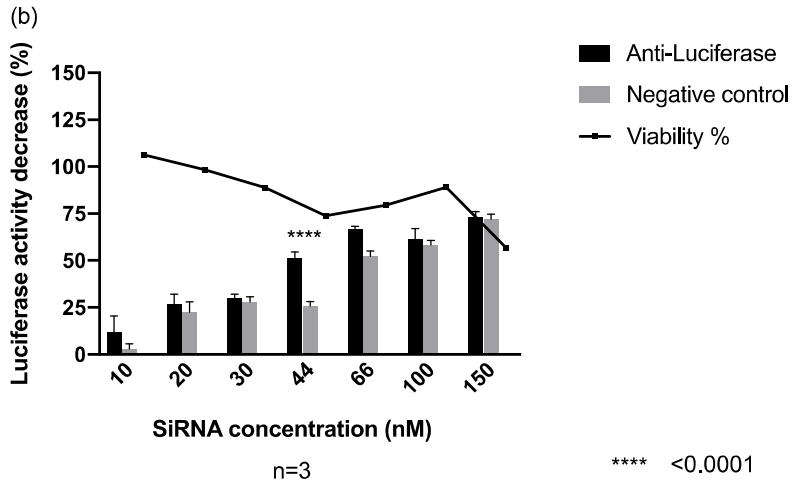

Figure 9. Cell viability and Luc silencing efficiency at various siRNA lipoplexe concentration. (a) Cytotoxicity was measured with the MTT test and expressed relatively to non-transfected cells (microfluidized lipoplexes of charge ratio 4-8, extrusion lipoplexes of charge ratio 4, siRNA concentration 10nM-150nM). (b) Luciferase silencing efficiency of microfluidized lipoplexes (charge ratio = 8) expressed as percentage of control non-transfected cells (mean +/- SD; n=3).

5. Conclusions

Overall, we have identified a cationic liposome preparation obtained by microfluidization combined with thin film hydration method which, at a lipoplexes charge ratio of 8, leads to gene silencing efficiency comparable to the more classical extrusion technique. The cytotoxicity was similar as compared to reference lipoplexes obtained by extrusion. In the present study, PEG lipid was used to decrease the size of liposomes and increase blood circulation time for further *in vivo* use. However, PEGylated lipids might also limit the silencing efficiency of the present lipoplexe formulation. Indeed, the lipid-PEG shell is recognized to weaken the electrostatic adhesion between cationic liposomes and negatively charged cell membrane, thus decreasing endocytosis and lipoplexe transfection efficiency [35].

The present results provide device-design approach using a fitted DoE (with parameters constrained by the device as well as the chosen raw material) to produce cationic liposomes, using a microfluidization process which is lab-scalable and potentially meeting the scale-up industry requirements. The chosen methodology and its fitted design can be used for other and more recent nanocarriers formulation[10],[39]. Ultimately, the parameters of different size reduction methods with design[9], [10], [39] or without design [22] can be used to determine the key factor influencing the physicochemical characters and functions of nanoparticle formulations.

6. Acknowledgements

The authors would like to thank Anne-Marie Lachages in UTCBS of Paris Descartes University for the helps of instructing the in vitro part.

References

[1] Paulson, H., 2006. RNA interference as potential therapy for neurodegenerative disease: applications to inclusion-body myositis? Neurology. 66, S114-7.

[2] Fire, A., Xu S., Montgomery, MK., Kostas, S.A., Driver, S.E., Mello, C.C., 1998. Potent and specific genetic interference by double-stranded RNA in Caenorhabditis elegans. Nature. 391, 806-11.

[3] Schlegel, A., Bigey, P., Dhotel, H., Scherman, D., Escriou, V., 2013. Reduced in vitro and in vivo toxicity of siRNA-lipoplexes with addition of polyglutamate. J Control Release. 165, 1-8.

[4] Adams, D., Gonzalez-Duarte, A., O'Riordan, W.D., Yang, C.C., Ueda, M., Kristen, A.V., Tournev, I., Schmidt, H.H., Coelho, T., Berk, J.L., Lin, K.P., Vita, G., Attarian, S., Planté-Bordeneuve, V., Mezei, M.M., Campistol, J.M., Buades, J., Brannagan, T.H. 3rd, Kim, B.J., Oh, J., Parman, Y., Sekijima, Y., Hawkins, P.N., Solomon, S.D., Polydefkis, M., Dyck, P.J., Gandhi, P.J., Goyal, S., Chen, J., Strahs, A.L., Nochur, S.V., Sweetser, M.T., Garg, P.P., Vaishnaw, A.K., Gollob, J.A., Suhr, O.B., 2018. Patisiran, an RNAi Therapeutic, for Hereditary Transthyretin Amyloidosis. N Engl J Med. 379, 11-21.

[5] Kumar, M., Bishnoi, R.S., Shukla, A.K., Jain, C.P., 2019. Techniques for Formulation of Nanoemulsion Drug Delivery System: A Review. Prev Nutr Food Sci. 24, 225-234.

[6] Ganesan, P., Karthivashan, G., Park, S.Y., Kim, J., Choi, D.K., 2018. Microfluidization trends in the development of nanodelivery systems and applications in chronic disease treatments. Int J Nanomedicine. 13, 6109-6121.

[7] Roces, C.B., Lou, G., Jain, N., Abraham, S., Thomas, A., Halbert, G.W., Perrie, Y., 2020. Manufacturing Considerations for the Development of Lipid Nanoparticles Using Microfluidics. Pharmaceutics. 12, 1095.

[8] Anderluzzi, G., Lou, G., Su, Y., Perrie, Y., 2019. Scalable Manufacturing Processes for Solid Lipid Nanoparticles. Pharm Nanotechnol. 7, 444-459.

[9] Vo, A., Feng, X., Patel, D., Mohammad, A., Kozak, D., Choi, S., Ashraf, M., Xu, X., 2020. Factors affecting the particle size distribution and rheology of brinzolamide ophthalmic suspensions. Int J Pharm. 30, 119495.

[10] Liu, H., Rivnay, B., Avery, K., Myung, J.H., Kozak, D., Landrau, N., Nivorozhkin, A., Ashraf, M., Yoon, S., 2020. Optimization of the manufacturing process of a complex amphotericin B liposomal formulation using quality by design approach. Int J Pharm. 30, 119473.

[11] Gala, R.P., Khan, I., Elhissi, A.M., Alhnan, M.A., 2015. A comprehensive production method of self-cryoprotected nano-liposome powders. Int J Pharm. 486, 153-8.

[12] Ong, S.G., Chitneni, M., Lee, K.S., Ming, L.C., Yuen, K.H., 2016. Evaluation of Extrusion Technique for Nanosizing Liposomes. Pharmaceutics. 8, 36.

[13] Jiang, T., Liao, W., Charcosset, C., 2020. Recent advances in encapsulation of curcumin in nanoemulsions: A review of encapsulation technologies, bioaccessibility and applications. Food Res Int. 132:109035.

[14] Kaps, L., Schuppan, D., 2020. Targeting Cancer Associated Fibroblasts in Liver Fibrosis and Liver Cancer Using Nanocarriers. Cells. 9, 2027.

[15] Akinc, A., Goldberg, M., Qin, J., Dorkin, J.R., Gamba-Vitalo, C., Maier, M., Jayaprakash, K.N., Jayaraman, M., Rajeev, K.G., Manoharan, M., Koteliansky, V., Röhl, I., Leshchiner, E.S., Langer, R., Anderson, D.G., 2009. Development of lipidoid-siRNA formulations for systemic delivery to the liver. Mol Ther. 17, 872-9.

[16] Byk, G., Dubertret, C., Escriou, V., Frederic, M., Jaslin, G., Rangara, R., Pitard, B., Crouzet, J., Wils, P., Schwartz, B., Scherman, D., 1998. Synthesis, activity, and structure--activity relationship studies of novel cationic lipids for DNA transfer. J Med Chem. 41, 229-235.

[17] Byk, G., Scherman, D., Schwartz, B., Dubertret, C., 2001. Lipopolyamines as transfection agents and pharmaceutical uses thereof. US Patent No. 6171612.

449 [18] Rhinn, H., Largeau, C., Bigey, P., Kuen, R.L., Richard, M., Scherman, D., Escriou,
450 V., 2009. How to make siRNA lipoplexes efficient? Add a DNA cargo. Biochim Biophys
451 Acta. 1790, 219-230.

452 [19] Schlegel, A., Largeau, C., Bigey, P., Bessodes, M., Lebozec, K., Scherman, D.,
453 Escriou, V., 2011. Anionic polymers for decreased toxicity and enhanced in vivo delivery
454 of siRNA complexed with cationic liposomes. J Control Release. 152, 393-401.

455 [20] Mignet, N., Richard, C., Seguin, J., Largeau, C., Bessodes, M., Scherman, D., 2008.
456 Anionic pH-sensitive pegylated lipoplexes to deliver DNA to tumors. Int J Pharm.
457 361,194-201.

458 [21] Microfluidizer LV1 Brochure, 2020. https://www.microfluidics-mpt.com/(accessed
459 01 Feb. 2020).

460 [22] Schuh, R.S., Poletto, É., Fachel, F.N.S., Matte, U., Baldo, G., Teixeira, H.F., 2018.
461 Physicochemical properties of cationic nanoemulsions and liposomes obtained by
462 microfluidization complexed with a single plasmid or along with an oligonucleotide:
463 Implications for CRISPR/Cas technology. J Colloid Interface. 530, 243-255.

464 [23] Thakkar, H.P., Baser, A.K., Parmar, M.P., Patel, K.H., Ramachandra, Murthy. R.,
465 2012. Vincristine-sulphate-loaded liposome-templated calcium phosphate nanoshell as
466 potential tumor-targeting delivery system. J Liposome Res. 22, 139-147.

467 [24] Yeo, L.K., Chaw, C.S., Elkordy, A.A., 2019. The Effects of Hydration Parameters
468 and Co-Surfactants on Methylene Blue-Loaded Niosomes Prepared by the Thin Film
469 Hydration Method. Pharmaceuticals (Basel), 12, 46.

470 [25] Danaei, M., Dehghankhold, M., Ataei, S., Hasanzadeh Davarani, F., Javanmard, R.,
471 Dokhani, A., Khorasani, S., Mozafari, M.R., 2018. Impact of Particle Size and
472 Polydispersity Index on the Clinical Applications of Lipidic Nanocarrier
473 Systems. Pharmaceutics. 10, 57.

474 [26] Kumar, A., Dixit, C.K., 2017. Methods for characterization of nanoparticles,
475 advances in Nanomedicine for the Delivery of Therapeutic Nucleic Acids. Woodhead
476 Publishing., England, 43-58.

477 [27] Honary, S., Zahir, F., 2013. Effect of Zeta Potential on the Properties of Nano-Drug
478 Delivery Systems-A Review (Part 2). Tropical Journal of Pharmaceutical Research. 12,
479 265-273.

480 [28] Arruda, D.C., Gonzalez, I.J., Finet, S., Cordova, L., Trichet, V., Andrade,
481 G.F., Hoffmann, C., Bigey, P., de Almeida Macedo, W.A., Da Silva Cunha A
482 Jr., Malachias de Souza, A., Escriou, V., 2019.
483 Modifying internal organization and surface morphology of siRNA lipoplexes by sodium
484 alginate addition for efficient siRNA delivery. J Colloid Interface Sci. 540, 342-353.

485 [29] Xu, R., He, X., 2016. Kinetics of a Multilamellar Lipid Vesicle Ripening:
486 Simulation and Theory. J Phys Chem B. 120, 2262-2270.

487 [30] Jain, A., Hurkat, P., Jain, S.K., 2019. Development of liposomes using formulation
488 by design: Basics to recent advances. Chem Phys Lipids. 224, 104764.

489 [31] Tirosh, O., Barenholz, Y., Katzhendler, J., Priev, A., 1998. Hydration of
490 polyethylene glycol-grafted liposomes. Biophys J. 74, 1371-1379.

491 [32] Frank, L., Sorgi Leaf, Huang., 1996. Large scale production of DC-Chol cationic
492 liposomes by microfluidization. Int J Pharm. 144, 131-139.

493 [33] Scherman, D., 2019. Advanced Textbook On Gene Transfer, Gene Therapy And
494 Genetic Pharmacology: Principles, Delivery And Pharmacological And Biomedical
495 Applications Of Nucleotide-based Therapies (Second Edition). World Scientific.,
496 Singapore, 263-264.

497 [34] Safinya, C.R., Ewert, K.K., Majzoub, R.N., Leal, C., 2014. Cationic liposome-
498 nucleic acid complexes for gene delivery and gene silencing. New J Chem. 38, 5164-
499 5172.

500 [35] Düzgüneş, N., Nir, S., 1999. Mechanisms and kinetics of liposome-cell
501 interactions. Adv Drug Deliv Rev. 40, 3-18.

502 [36] Gill, K.K., Kaddoumi, A., Nazzal, S., 2015. PEG-lipid micelles as drug carriers:
503 physiochemical attributes, formulation principles and biological implication. J Drug
504 Target. 23, 222-31.

505 [37] Constantinescu CA, Fuior EV, Rebleanu D, Deleanu M, Simion V, Voicu G, Escriou
506 V, Manduteanu I, Simionescu M, Calin M., 2019. Targeted Transfection Using
507 PEGylated Cationic Liposomes Directed Towards P-Selectin Increases siRNA Delivery
508 into Activated Endothelial Cells. Pharmaceutics. 11:47.

509 [38] Technical bulletin, Luciferase Assay System 2019. http://www.promega.com/
510 (accessed 01 Dec. 2019).

511 [39] Penoy N, Grignard B, Evrard B, Piel G., 2021. A supercritical fluid technology for
512 liposome production and comparison with the film hydration method. Int J Pharm.
513 592:120093.

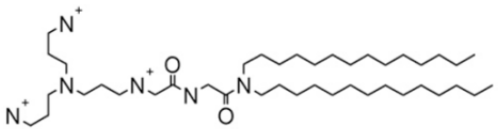

DMAPAP

Synthesized cationic lipid

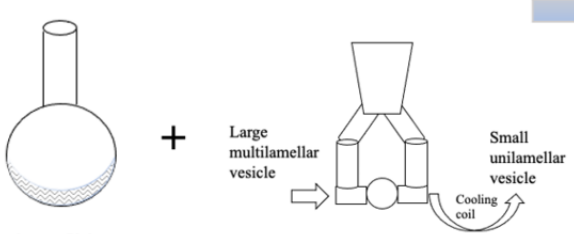

Thin film hydration

Microfluidization

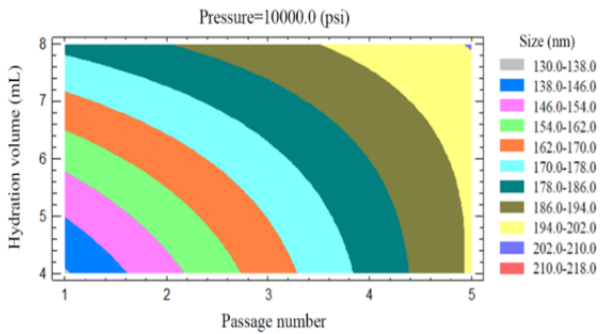

Design of Experiment (DOE)

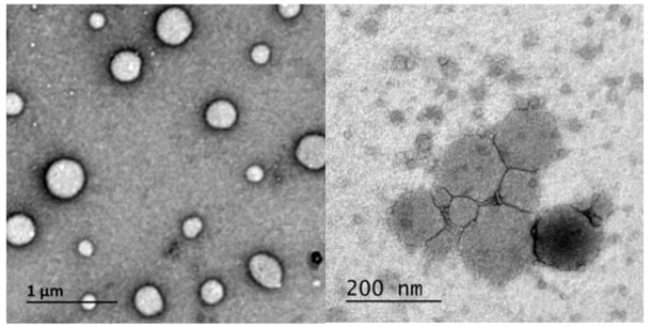

siRNA-lipoplexes

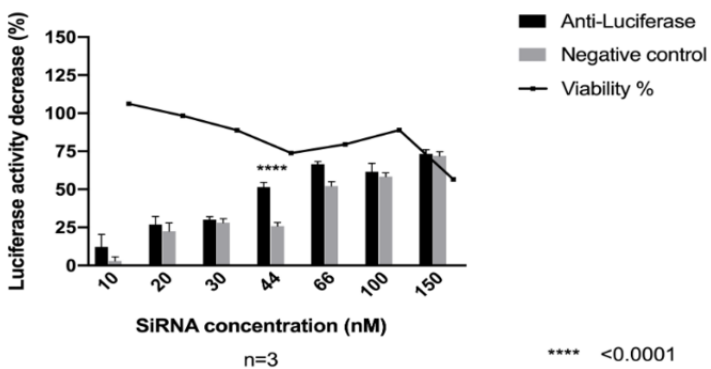

In-vitro tests